Journal of Pharmaceutical and Biomedical Analysis 72 (2013) 231–239

Contents lists available at SciVerse ScienceDirect

Journal of Pharmaceutical and Biomedical Analysis

journal homepage: www.elsevier.com/locate/jpba

Correlation between structure, retention, property, and activity of biologically relevant 1,7-bis(aminoalkyl)diazachrysene derivatives

Sandra Šegan[a], Jelena Trifković[b], Tatjana Verbić[b], Dejan Opsenica[a], Mario Zlatović[b], James Burnett[c], Bogdan Šolaja[b], Dušanka Milojković-Opsenica[b,*]

[a] Institute of Chemistry, Technology and Metallurgy, University of Belgrade, Njegoševa 12, 11000 Belgrade, Serbia
[b] Faculty of Chemistry, University of Belgrade, P.O. Box 51, 11158 Belgrade, Serbia
[c] Target Structure-Based Drug Discovery Group, SAIC-Frederick, Inc., National Cancer Institute at Frederick, P.O. Box B, Frederick, MD, United States

ARTICLE INFO

Article history:
Received 13 June 2012
Received in revised form 19 August 2012
Accepted 21 August 2012
Available online 27 August 2012

Keywords:
1,7-Bis(aminoalkyl)-diazachrysene derivatives (1,7-DAAC)
Lipophilicity
Acidity constants
Quantitative structure–retention relationship (QSRR)
Quantitative structure–activity relationship (QSAR)

ABSTRACT

The physicochemical properties, retention parameters (R_M^0), partition coefficients ($\log P_{OW}$), and pK_a values for a series of thirteen 1,7-bis(aminoalkyl) diazachrysene (1,7-DAAC) derivatives were determined in order to reveal the characteristics responsible for their biological behavior. The investigated compounds inhibit three unrelated pathogens (the Botulinum neurotoxin serotype A light chain (BoNT/A LC), *Plasmodium falciparum* malaria, and Ebola filovirus) *via* three different mechanisms of action. To determine the most influential factors governing the retention and activities of the investigated diazachrysenes, R_M^0, $\log P_{OW}$, and biological activity values were correlated with 2D and 3D molecular descriptors, using a partial least squares regression. The resulting quantitative structure–retention (property) relationships indicate the importance of descriptors related to the hydrophobicity of the molecules (*e.g.*, predicted partition coefficients and hydrophobic surface area). Quantitative structure–activity relationship models for describing biological activity against the BoNT/A LC and malarial strains also include overall compound polarity, electron density distribution, and proton donor/acceptor potential. Furthermore, models for Ebola filovirus inhibition are presented qualitatively to provide insights into parameters that may contribute to the compounds' antiviral activities. Overall, the models form the basis for selecting structural features that significantly affect the compound's absorption, distribution, metabolism, excretion, and toxicity profiles.

1. Introduction

Physicochemical screens are increasingly being used during the early stages of drug discovery to provide a more comprehensive understanding of the key properties that affect the biological disposition (*i.e.*, ADME—absorption, distribution, metabolism, and excretion) of promising leads [1,2]. The most commonly measured physicochemical properties are permeability and solubility (due to their importance in the gastrointestinal absorption of orally administered drugs), and lipophilicity, pK_a, integrity, and stability (as these properties generally affect the pharmaceutical potential of a compound).

Lipophilicity is a fundamental property of compounds that serves as a benchmark for predicting solubility, permeability, and protein binding [2], as it is indicative of a compound's preference for van der Waals interactions with other molecules *versus* hydrogen bonds or polar interactions with water and protein receptors. The lipophilicity is usually expressed as a logarithm of partitioning between 1-octanol and water ($\log P_{OW}$) [3]. The Organization for Economic Co-operation and Development (OECD) Guidelines for the Testing of Chemicals [4], Test 117, describes a method for determination of $\log P_{OW}$ using reversed-phase high performance liquid chromatography (RPHPLC). In several publications the HPLC method is substituted with thin-layer chromatography (TLC) [5], keeping the same principles as in Test 117, with RP-18 stationary phase and the composition of the mobile phase that provide optimal selectivity. The advantages of RPTLC method are: (1) only a small amount of sample is needed for estimation, (2) low sensitivity to impurities, (3) rapid determination, (4) good accuracy and reproducibility, and (5) greater applicability to compounds with higher lipophilicity [6]. Thus, the RPTLC enables determination of a retention parameter, R_M^0 [7], which reflect the partition of the compound between non-polar stationary phase and polar aqueous mobile phase, thereby enabling the estimation of the lipophilicity of the tested compounds.

A second compounds' descriptor—the ionization coefficient (represented by the acidity constant pK_a), is also pivotal for estimating the physicochemical behavior of compounds and their

* Corresponding author. Tel.: +381 11 3336766; fax: +381 11 2639357.
E-mail address: dusankam@chem.bg.ac.rs (D. Milojković-Opsenica).

0731-7085/$ – see front matter © 2012 Elsevier B.V. All rights reserved.
http://dx.doi.org/10.1016/j.jpba.2012.08.025

distribution over a pH gradient. Determination of pK_a values rely on the measurement of any physical property that varies with protonation [8]. Over the past few decades, it has been found that potentiometric and spectrophotometric determination, although among the oldest of methods, are the most useful in this capacity, as simple equipment and solutions are used [9].

Quantitative structure–retention relationship (QSRR) and quantitative structure activity (property) relationship (QSA(P)R) models correlate solute molecular structures, to their chromatographic behavior, *i.e.* their pharmaco-biochemical activities. For such studies, mathematical models are developed to facilitate the prediction of activities, or properties, of compounds that have not yet been synthesized or examined in *in vitro* and/or *in vivo* experiments. These models can aid in rationalizing hypotheses for the mechanism of compound–receptor binding [10,11].

Recently, a series of 1,7-diazachrysene (1,7-DAAC)-based derivatives were synthesized and determined to be potent inhibitors of three unrelated pathogens: the BoNT/A LC, a Zn(II) metalloprotease (which causes the paralysis associated with botulism), *Plasmodium falciparum* (which causes malaria), and Ebola filovirus (EBOV) (which causes hemorrhagic fever) [12,13]. With respect to mode of action, three different mechanisms are employed, thus demonstrating the unique antipathogenic potential of this chemotype. Hence, based on the significant and diverse biological activities of the indicated compounds, they form an ideal test set for further determination of the fundamental chemical characteristics responsible for their behavior in the biological environment.

The goals of this study were: (i) to experimentally determine the physicochemical properties, retention parameter (R_M^0), and partition coefficient ($\log P_{OW}$) as measures of lipophilicity, as well as pK_a values, for the series of indicated 1,7-DAAC derivatives (*vide supra*), and (ii) to determine the compound's 2D and 3D molecular descriptors, and in conjunction with their physicochemical parameters and empirical biological data [12], use multivariate statistical analysis (principal component analysis and partial least square regression) to determine crucial factors governing retention and activity to propose structural features that contribute to the ADME-Tox profiles for the compounds.

2. Experimental

2.1. Reagents

The synthesis and characterization of the studied 1,7-DAAC derivatives (Table 1) has been reported [12].

All standard compounds were purchased from Aldrich (Milwaukee, WI, USA), Fluka (Buchs, Switzerland), or Merck (Darmstadt, Germany), while their experimentally determined $\log P_{OW}$ values were obtained from the literature [14]. Standards were chosen based on their structural similarity to the investigated 1,7-DAAC derivatives. The optimal range of $\log P_{OW}$ values was considered broad enough to provide reliable regression performance ($1-4\log P_{OW}$ units). The following nine compounds with known $\log P_{OW}$ values (provided in parentheses) were selected as standards (mainly naphthalene and quinoline

Table 1
Experimentally determined parameters of lipophilicity and biological activity for investigated compounds **1**–**13**.

Comp.	R_M^0 [b]	$\log P_{OW}$	Biological activity[a]			
			BoNT/A LC (%)	D6 IC_{50} (nM)	W2 IC_{50} (nM)	C235 IC_{50} (nM)
1	2.29	4.24	55.6	5.23	2.00	8.05
2	3.41	5.39	73.5	14.84	7.75	34.29
3	2.18	3.88	39.0	5.93	6.13	9.84
4	3.02	5.13	60.3	16.76	8.11	25.9
5	2.29	4.00	72.3	1029.42	345.68	1027.45
6	3.15	5.66	68.9	103.47	352.71	54.82
7	3.75	5.80	64.7	30.01	8.65	66.5
8	3.06	4.74	63.4	8.79	5.50	10.55
9	3.49	5.39	66.1	9.26	6.98	24.84
10	2.91	5.13	55.4	6.01	3.48	3.32
11	2.56	4.49	57.0	15.61	9.19	15.27
12	1.76	3.51	62.7	270.29	871.25	1021.04
13	2.09	4.12	70.0	708.29	1701.59	2030.86

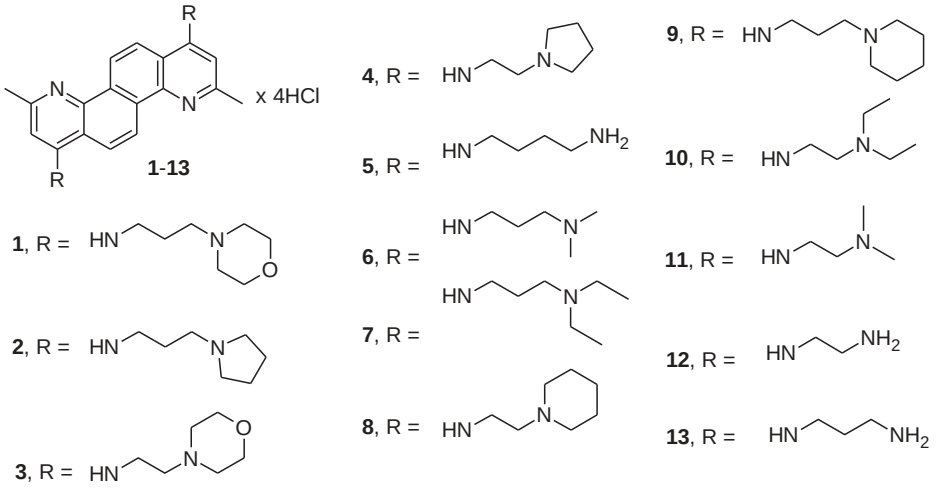

[a] Taken from Ref. [12].
[b] R_M^0 = retention parameter.

derivatives with alkyl chain nitrogen or oxygen atoms): chloroquine (3.03), AQ2—*N*-(7-chloroquinolin-4-yl)ethane-1,2-diamine (1.44), AQ3—*N*-(7-chloroquinolin-4-yl)propane-1,3-diamine (1.93), hydroquinone (0.59), 2-naphthol (2.84), 4-*t*-butylphenol (3.31), diphenylamine (3.50), benzophenone (3.18), and naphthalene (3.29).

Tetrahydrofuran (THF), used as an organic modifier in mobile phases, was of analytical reagent grade and purchased from Merck (Darmstadt, Germany). Water was purified using a water purification system Millipore Simplicity 185 S.A., 67120 (Molshem, France).

2.1.1. Potentiometry

All chemicals were of analytical reagent grade, and were purchased from Merck (Darmstadt, Germany). Solutions of NaOH and HCl (0.1 M) were prepared in deionized water and potentiometrically standardized. Working solutions of 1,7-DAAC derivatives (as tetra HCl salts) were prepared in 0.1 M NaCl ($c_{1,7\text{-DAAC}} = (0.8–1.0) \times 10^{-3}$ M).

2.1.2. UV/Vis spectrophotometry

A stock solution of derivative **12** (Table 1) ($c = 5 \times 10^{-3}$ M) was prepared in 0.1 M NaCl. Working solutions ($c = 5 \times 10^{-5}$ M) were prepared in appropriate buffer solutions in pH range 4.0–10.2 (I = 0.1 M (NaCl)). Acetate buffers were used for pH range 4.0–6.0, phosphate buffers for pH 6.1–8.0, borate buffers for pH 8.1–9.3, and carbonate buffers for pH 9.4–10.2 ($c^{\text{tot}}_{\text{buff}} = 0.01\,M$).

2.2. Apparatus and methods

The chromatographic investigations were performed on commercially available octadecyl silica plates (RP-18 W F_{254s}, Art. 5559, Merck, Darmstadt, Germany) with mobile phase THF–NH_3–H_2O. The content of THF was changed in interval of 60–80 vol% in steps of 5% while the content of NH_3 was kept constant at 5 vol%. The plates (10 cm × 10 cm) were spotted with 1.0 μL aliquots of freshly prepared solutions of the investigated substances in water.

Compounds used as standards were dissolved in methanol and chromatographed together with 1,7-DAAC-based derivatives using mobile phase THF–NH_3–H_2O (75:5:20, v/v/v).

Chromatography was performed in an HPTLC developing chamber (Camag, Muttenz, Switzerland) in the tank configuration. Before development, the spotted plates were equilibrated for 15 min in a chromatographic chamber saturated with the vapor of the mobile phase being used. Detection of individual zones was performed using a UV lamp (254 nm). All experiments were done at room temperature.

Potentiometric titrations were performed using a TTT-60 titrator equipped with an ABU-12 autoburette (Radiometer Copenhagen, Denmark), and pH was measured with a PHM240 pH-Meter (Radiometer) with a combined GK2401B electrode (Radiometer).

Acidity constants of ten 1,7-DAAC derivatives were potentiometrically determined in aqueous media at constant ionic strength (I = 0.1 M (NaCl)) and at $t = 25 \pm 1$ °C. Prior to titration, 200 μL of the standard 0.1 M HCl solution was added to 14.00 mL of working compound solution ($c = (0.8–1.0) \times 10^{-3}$ M). All probes were titrated with 5 μL increments of the standard 0.1 M NaOH solution. Measured pH values were converted to pc_H according to the relation: $pc_H = -\log[H_3O^+] = pH - A$, where A is the correction factor (A = 0.10) as determined by the potentiometric titration of the standard HCl solution with the standard NaOH solution under experimental conditions [15]. The pK_w value (pK_w 13.75 ± 0.01) was calculated from the same set of titrations. HyperQuad 2008 [16] software was used to evaluate the dissociation scheme in the studied pc_H range and to calculate the values of acidity constants from three to six repeated titrations.

UV/Vis spectra were recorded on a GBC Cintra 6 spectrophotometer (GBC Dandenong, Australia) with a 1 cm quartz cuvette. All spectra were recorded against the corresponding blank (appropriate buffer solution) in the 220–500 nm wavelength range, with a 500 nm/min scan rate.

2.3. Software

Compound lipophilicity was predicted using the program *C* log *P* working with the Hansch–Leo's fragment constant method [17] available through Biobyte (http://www.biobyte.com). Calculated pK_a values were obtained using Epik module version 2.2 from Schrödinger Suite 2011 [18], with water at pH 7.0 as the solvent. For pK_a prediction, a sequential pK_a mode that predicted pK_a for successive protonation/deprotonation of the molecule was used. The pK_a values were adjusted after the addition (removal) of each proton.

All molecules were built using the Maestro interface of Schrödinger Suite 2010 (Maestro, version 9.1, Schrödinger, LLC, New York, NY, 2010). To gain a more thorough understanding of the spatial properties and behavior of the examined molecules, Conformational search from the MacroModel module (version 9.8) in Schrödinger Suite 2010 was employed. All molecules were tetraprotonated. The OPLS_2005 force field, with water as the solvent, and using the mixed MCMM/low-mode conformational search method [19], were the set parameters. Every conformation was minimized using the Polak–Ribiere conjugate gradient method [20], with 1000 maximum iterations or until a 0.05 convergence threshold was obtained. Duplicates were removed and all structures within energy window of 21 kJ/mol were saved. Diverse conformations within a small energy window were produced following the procedure indicated above, and represent dynamic equilibrium between borderline conformations (Fig. 1).

The following software was used for the calculation of molecular descriptors: QikProp (version 3.3, Schrödinger, 2010) for physically significant descriptors and pharmaceutically relevant properties, and MOPAC 7.1 single point calculations with the RM1 method [21] for semiempirical parameters. Based on the calculated results, a data table used for QSRR, QSPR, and QSAR modeling was designed (Table S1, Supplementary material).

2.4. Multivariate statistical analysis and modeling

Principal component analysis (PCA) and Hierarchical cluster analysis (HCA) were performed using PLS_Toolbox statistical package (version 5.7, Eigenvectors Inc.) from MATLAB version 7.4.0.287 (R2007a) (MathWorks INC, Natick, MA, USA). Partial least square (PLS) were performed using TOMCAT, a Matlab toolbox for multivariate calibration techniques [22]. PCA was carried out as an exploratory data analysis by using a singular value decomposition algorithm (SVD) and a 0.95 confidence level for Q and T^2 Hotelling limits for outliers. An agglomerative HCA was performed in addition to PCA to group similar objects more easily and further clarify PCA results. Specifically, HCA considers all the data variability, while PCA performs an account of the loss of information. The best results for HCA were obtained using the Ward method to calculate cluster distances and by applying Euclidean distance as a measure of distance between the samples. The PLS method calculates latent variables for both independent and dependent variable matrices plus a relationship between them. Validation of the models was performed using Monte-Carlo cross-validation (MCVV) [23]. MCCV is an effective method for determining the number of components in the calibration model for a small data set. Unlike leave-one-out procedure it can avoid an unnecessary large model and therefore decreases the risk of over-fitting for the calibration model.

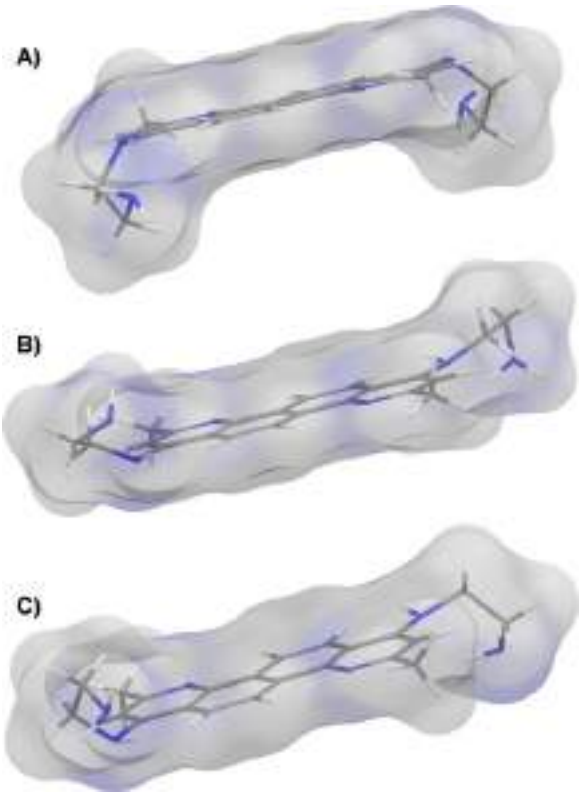

Fig. 1. Different borderline conformations of compound **12** with small differences in potential energies: (a) −371.18 kJ/mol; (b) −369.44 kJ/mol; (c) −368.48 kJ/mol.

By default the number of iterations is set to be twice the number of objects in the data [22]. The quality of the models was monitored with the following parameters: (1) R^2_{cal}(cum), the cumulative sum of squares of the Ys explained by all extracted components, and R^2_{CV}(cum), the cumulative fraction of the total variation of the Ys that can be predicted by all extracted components—these two values should be as high as possible, and (2) *RMSEC* (Root Mean Square Errors of Calibration) and *RMSECV* (Root Mean Square Errors of Cross-Validation)—these values should be as low as possible, and with the lowest difference between the two [24,25].

The data were mean-centered and scaled to unit variance before statistical analyses. Autoscaling of the data was chosen as a pretreatment method in order to prevent highly abundant components from dominating components present in much smaller quantities. The R^0_M, and $\log P_{OW}$ values, *i.e.* values for the inhibition of the BoNT/A LC, malaria, and EBOV as dependent variables in the QSR(P)R, *i.e.* QSAR equations, were regressed against the molecular structural descriptors (independent variables).

3. Results and discussion

3.1. Physicochemical properties. Lipophilicity of the investigated compounds

1,7-DAAC derivatives possess two mutual chemical components that can participate in chromatographic interactions: a diazachrysene aromatic core and either bis(aminoalkyl) or bis polar (morpholine) side-chain substituents (Table 1). The presence of the highly polarized π-electron system in the diazachrysene core offers the possibility for dipolar interactions between the molecules, as well as interactions with both stationary and mobile phases, while the bis(alkyl) and bis(morpholine) nitrogen atoms behave as proton acceptors.

Considering the large diversity of 1,7-DAAC derivative conformations generated by the employed computational search procedure (see Section 2.3), and small energy difference between the conformations, regardless of shape and surface exposure, it can be postulated that, at room temperature, there is no significant energy barrier to side-chain rotation. Thus, it can be assumed that the examined compounds would be adsorbed on the non-polar stationary phase predominantly in the conformation with the largest hydrophobic surface exposed to adsorbent. In this regard, it can also be assumed that the prevailing conformations are those with both of the compound's side-chains oriented on the same side of the diazachrysene aromatic core (Fig. 1a).

Since the diazachrysene component of all of the studies derivatives (Table 1), differences in retention were dependent on both the number of methylene groups in the compound's aminoalkyl side-chains (two, three or four) and the structure of aminoalkyl side-chain terminal substituents (*N*,*N*-dimethyl, *N*,*N*-diethyl, pyrrolidine, piperidine, morpholine or primary amines). R^0_M values of the 1,7-DAAC derivatives obtained by extrapolation of R_M values to 0 vol% of organic solvent are summarized in Table 1. Within each group, an increase of the number of C-atoms in the aliphatic, methylene side-chains strengthens the retention of the compounds due to stronger hydrophobic interactions with the stationary phase. In addition, the terminal component nitrogen atoms can act as proton acceptor and/or donating centers that interact with both the mobile and the stationary phases. Taking into account the retention of different groups of amines, it can be concluded that primary amines (**5**, **12**, **13**) exhibit the weakest retention, while the tertiary amines (**6**, **7**, **10**, and **11**) exhibit the strongest retention. Pyrrolidine (**2** and **4**) and piperidine derivatives (**8** and **9**) show similar retention to tertiary amines, whereas the retention of morpholine derivatives (**1** and **3**) is similar to those of primary amines. In general, it was observed that the R^0_M values show linear dependence on THF concentration in the mobile phase.

The $\log P_{OW}$ of the investigated compounds was experimentally determined by simultaneous chromatographing with standards. Partition coefficients were correlated with R_M values (presented in parentheses: chloroquine (0.03), AQ2 (−0.23), AQ3 (−0.19), hydroquinone (−0.48), 2-naphthol (−0.18), 4-*t*-butylphenol (−0.10), diphenylamine (−0.02), benzophenone (−0.05), and naphthalene (0)). Linear regression of the calibration data gives Eq. (1):

$$R_M = -0.502 + 0.143\ \log P_{OW}$$
$$r = 0.914,\ N = 9,\ s = 0.069,\ P = 5.650 \times 10^{-4} \quad (1)$$

$\log P_{OW}$ values of the 1,7-DAAC derivatives were calculated by substituting the R_M values into Eq. (1) and listed in Table 1. Experimentally established $\log P_{OW}$ values were compared with $C\log P$ (a computationally determined $\log P$ value that correlates with R^0_M) [26] and QP $\log P_{O/W}$ values. The statistically significant linear correlations were obtained ($r = 0.915$; $n = 13$, $t = 7.15$ ($t_{cr(0.05,11)} = 2.20$), $F = 51.21$, and $r = 0.822$; $n = 13$, $t = 4.80$, $F = 22.92$, respectively). These data provide evidence that chromatography can be used to determine the lipophilicity of the examined 1,7-DAAC derivatives.

Notably, the lipophilicity of the investigated compounds is in accordance with their chromatographic behavior. Propylamino and butylamino substituents provide increased lipophilicity *versus* corresponding ethyl derivatives. Lipophilicity also increases with increasing substitution on the side-chain basic nitrogens, *i.e.*, primary amine derivatives are less hydrophobic than those possessing *N*,*N*-dimethyls, *N*,*N*-diethyls, pyrrolidine, piperidine, and morpholine substituents. Additionally, the incorporation of terminal morpholine rings has a negative impact on lipophilicity, resulting in $\log P_{OW}$ values similar to those of primary amines. Namely, morpholine derivatives **1** and **3** were synthesized to investigate the influence of additional polar atom in aminoalkyl substituent,

Table 2
Experimentally determined (exp)[a] and calculated (Epik)[18] pK_a values of 1,7-DAAC derivatives in aqueous solution. I = 0.1 M (NaCl), t = 25 ± 1 °C.

Compound (concentration)	Determination method	pK_{a1} ± SD	pK_{a2} ± SD	pK_{a3} ± SD	pK_{a4} ± SD
12 (1.00×10^{-3} M)	exp	5.86 ± 0.05	7.70 ± 0.05	8.67 ± 0.05	9.83 ± 0.06
	Epik	6.7 ± 1.2	7.9 ± 1.2	9.0 ± 0.7	9.6 ± 0.7
11 (1.04×10^{-3} M)	exp	5.91 ± 0.02	7.58 ± 0.02	8.43 ± 0.03	–
	Epik	6.8 ± 1.2	8.0 ± 1.2	8.4 ± 1.2	9.0 ± 1.2
10 (1.00×10^{-3} M)	exp	5.87 ± 0.06	7.84 ± 0.06	8.70 ± 0.08	–
	Epik	6.8 ± 1.2	8.0 ± 1.2	8.4 ± 1.2	9.0 ± 1.2
13 (0.79×10^{-3} M)	exp	6.28 ± 0.03	8.59 ± 0.03	9.45 ± 0.04	–
	Epik	7.3 ± 1.2	8.4 ± 1.2	9.8 ± 0.7	10.4 ± 0.7
6 (0.80×10^{-3} M)	exp	6.33 ± 0.03	8.21 ± 0.02	–	–
	Epik	7.2 ± 1.2	8.4 ± 1.2	9.2 ± 1.2	9.8 ± 1.2
7 (1.03×10^{-3} M)	exp	6.18 ± 0.03	8.48 ± 0.03	9.42 ± 0.04	–
	Epik	7.2 ± 1.2	8.4 ± 1.2	9.2 ± 1.2	9.8 ± 1.2
2 (0.80×10^{-3} M)	exp	6.29 ± 0.03	8.57 ± 0.03	–	–
	Epik	7.2 ± 1.2	8.4 ± 1.2	10.1 ± 0.5	10.7 ± 0.5
9 (1.02×10^{-3} M)	exp	6.19 ± 0.03	8.39 ± 0.03	–	–
	Epik	7.2 ± 1.2	8.4 ± 1.2	9.5 ± 1.2	10.1 ± 1.2
1 (0.76×10^{-3} M)	exp	5.78 ± 0.01	6.43 ± 0.01	7.14 ± 0.01	–
	Epik	6.5 ± 1.2	7.1 ± 1.2	7.3 ± 0.6	8.5 ± 0.6
5 (1.04×10^{-3} M)	exp	6.47 ± 0.06	8.98 ± 0.05	9.43 ± 0.08	–
	Epik	7.5 ± 1.2	8.7 ± 1.2	9.9 ± 0.7	10.5 ± 0.7

[a] Experimentally determined pK_a values are given as mean values of three to six times repeated titrations.

capable to participate as non-basic H-bond acceptor (derivatives **1** and **3** *vs*. **8** and **9**). Compounds containing pyrrolidine ring in side-chain are more lipophilic than the derivatives with piperidine and *N*,*N*-diethyl groups. These results indicate that steric limitations for side-chain amino substitutions play an important role in the transport of the compounds through lipid membranes.

3.2. Study of protolytic equilibria

In aqueous media 1,7-DAAC derivatives act as weak bases, with four (out of six) potentially protonable nitrogen atoms at physiological pH (aniline nitrogens get protonated in extremely acidic media). Considering the calculated pK_a values (Table 2), it was expected that differences between the four consecutive pK_as that were studied would not be sufficient ($\Delta pK_a \geq 4$) for classical spectrophotometric determination [9]. Thus, potentiometric acid–base titration and HyperQuad 2008 [16] software were used for pK_a determination (Table 2). All four dissociation constants were determined only for the derivative **12**, which possesses $(CH_2)_2NH_2$ side-chains, and consequently exhibited the highest degree of solubility among the studied derivatives. For other examined 1,7-DAAC derivatives, two or three pK_a values were experimentally determined—as dictated by solubility.

As observed in Table 2, pK_{a1} and pK_{a2} values (which resulted in deprotonation of the aromatic nitrogens) are similar for derivatives with the same number of methylene groups in the side-chain. In general, pK_{a1} and pK_{a2} values increase with the number of methylene groups in the side-chains due to positive inductive effect of alkyl groups. The exception is derivative **1**, which possesses trimethylene side-chains, as well as the electronegative oxygen atom in the terminal morpholine rings. Hence, **1** has lower pK_{a1} and pK_{a2} values. Steric hindrance (which lowers pK_a values) and alkyl substituent inductive effects (which raise pK_as) are the main factors affecting pK_{a3} and pK_{a4} values (*i.e.*, terminal nitrogen atom protonation) for compounds providing sufficient solubility.

In order to validate the quality of the predicted pK_a values, experimentally obtained pK_as were also compared with calculated pK_as in Table 2. The student's paired *t*-test was used for the comparison and indicated that the differences between pK_{a1}s determined by these two methods were statistically significant (t = 29.92, $t_{cr(0.05,9)}$ = 2.26). However, application of the same test on pK_{a2} and pK_{a3} values indicated no statistically significant differences between predicted and calculated values (pK_{a2}: t = 1.36, $t_{cr(0.05,9)}$ = 2.26; pK_{a3}: t = 0.95, $t_{cr(0.05,6)}$ = 2.45, Table 2).

Based on the experimentally determined pK_{a1}–pK_{a4} values (Table 2), a representative distribution diagram of derivative **12** was calculated (Fig. 2). On the basis of this diagram, determination of the dominant protonated state at a given pH of interest is straightforward. For example, it was found that at pH 5.0, which is the estimated pH within the food vacuole of the *P. falciparum* parasite [27,28], the predominant species of **12** is BH_4^{4+} (88%), while BH_3^{3+} (12%) is the only other species present in solution. For comparison, at pH 7.4 (the pH of blood), a mixture of species was observed: BH_4^{4+} (2%); BH_3^{3+} (63%), BH_2^{2+} (33%), and BH^+ (2%).

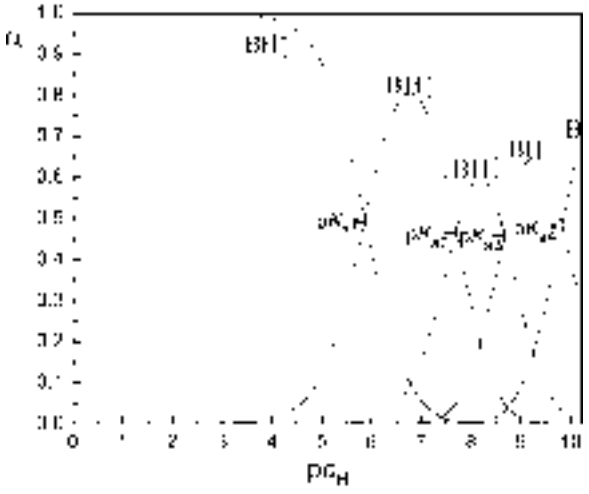

Fig. 2. Distribution diagram of 1,7-DAAC derivative **12**.

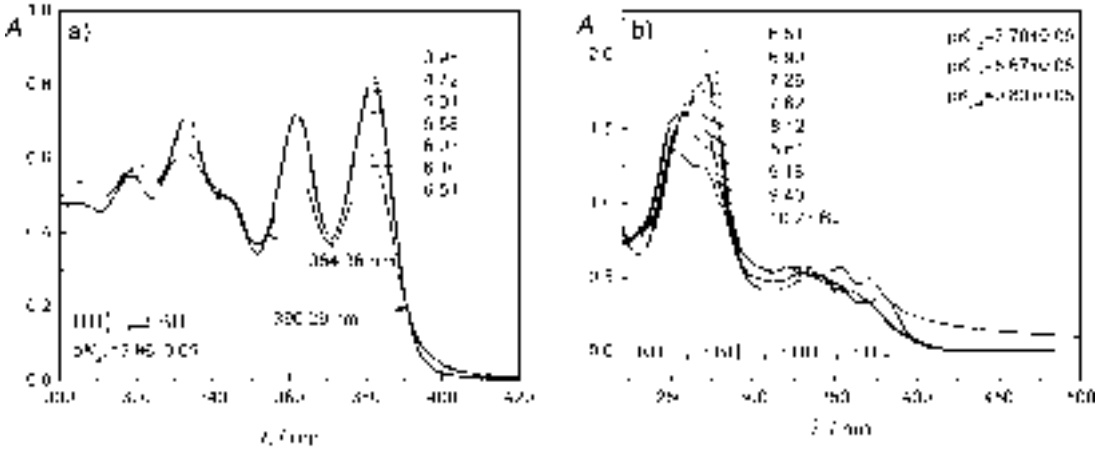

Fig. 3. (a) UV/Vis spectra of 1,7-DAAC derivative 12 ($c = 5 \times 10^{-5}$ M) in aqueous solutions, pH interval 3.98–6.51 (shown in the figure), with on-going dissociations and potentiometrically determined pK_a values indicated; $t = 25 \pm 1$ °C; scan rate 500 nm/min. (b) UV/Vis spectra of 1,7-DAAC derivative 12 ($c = 5 \times 10^{-5}$ M) in aqueous solutions, pH interval 6.51–10.23 (shown in the figure), with on-going dissociations and potentiometrically determined pK_a values indicated; $t = 25 \pm 1$ °C; scan rate 500 nm/min.

Spectral changes obtained in aqueous buffer solutions with pH ranging from 4.0 to 10.2 (Fig. 3) are in good agreement with obtained pK_a values for aqueous media. As observed in Fig. 3a, small but obvious differences are visible in the spectrum recorded in solution at pH 4.72 (comparing to pH 3.98); these data indicate initiation of the dissociation process. This is in good agreement with obtained pK_{a1} value (5.86 ± 0.05), as it is expected to uncover visible spectral differences in a solution with pH $\sim$ p$K_{a1} - 1$. Within pH range 3.98–6.50, isosbestic points are visible (λ 354.36 nm and 390.29 nm), therefore the dissociation of BH_4^{4+} dominates in solution. Following, as the pH increased (Fig. 3b), additional dissociation was observed. Furthermore, as differences between pK_{a2}, pK_{a3}, and pK_{a4} are not as pronounced as the difference between pK_{a1} and pK_{a2}, simultaneous dissociation of BH_3^{3+}, BH_2^{2+}, and BH^+ are occurring at the same time, and no isosbestic points are visible. At pH 10.23, where the dominating species is the non-ionized molecule (B, Fig. 3b), precipitation is obvious.

3.3. Principal component analysis

PCA was performed on retention data and on molecular descriptors in order to provide basic insights into similarities among the studied derivatives and to provide an overview of the data in order to remove outliers.

PCA derived on the initial chromatographic data (R_M values) using a covariance matrix with autoscaling, resulted in a two-component model that explained 99.23% of the total variances. The first principal component, PC1, accounted for 98.55% of data variance, and the second one, PC2, for 0.68%. Score values for PC1 and PC2 are shown in Fig. 4a. All the data fell within the Hotelling T^2 ellipse, suggesting that there are no outliers. In this regard, the results show that PC1 separates primary amines and morpholine derivatives from tertiary amines and pyrrolidine and piperidine derivatives. This classification of 1,7-DAAC derivatives is based on the ability of the compounds to engage in hydrogen bonding interactions (compounds **1**, **3**, **5**, **12**, **13** in comparison with compounds **2**, **4**, **6**–**11**). Specifically, along the PC1 axis the lipophilicity of the compounds increases: derivatives possessing the ability to form hydrogen bonds (compounds **1**, **3**, **5**, **12**, **13**) are located on the negative segment of the axis, derivatives possessing ethylene linkers (compounds **1**, **4**, **8**, **10**) are located in the middle of the PC score graph, and the most lipophilic derivatives with propylamino linkers (compounds **2**, **6**, **7**, **9**) are positioned on the positive segment of the graph. Furthermore, the obtained clustering is confirmed by the HCA presented in Fig. 5a. Regarding to dendrogram, the compounds were divided into two clusters with similar lipophilicity characteristics. Within the second cluster, substances are grouped into two classes according to the number of methylene groups in their aminoalkyl substituents.

PCA of the descriptors resulted in a four-component model that explains 91.91% of the total variance. Hence, PCA and HCA revealed different derivative classifications (Figs. 4b and 5b, respectively).

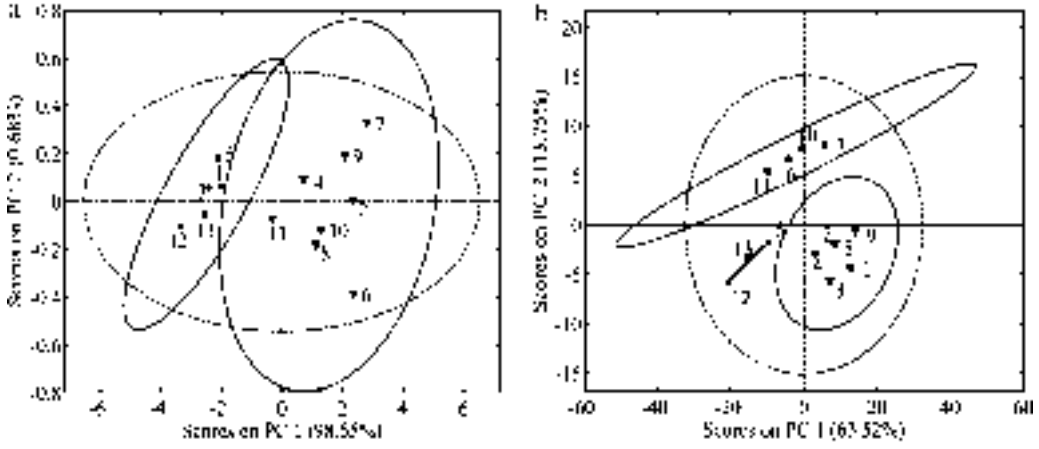

Fig. 4. PCA scores: (a) chromatographic data, (b) molecular descriptors.

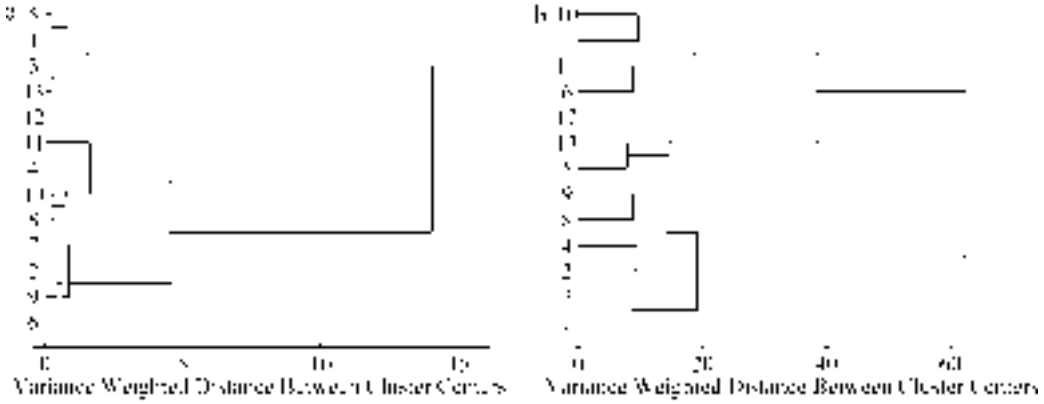

Fig. 5. Cluster analysis: (a) chromatographic data, (b) molecular descriptors.

Samples were clustered into three main groups, with primary amines in one group, tertiary amines in a second, and compounds possessing terminal cyclic aminoalkyl substituents in a third. Interestingly, in the case of HCA, within the third cluster, three separate classes are formed in accordance with the presence of pyrrolidine, piperidine, or morpholine substituents. Observing the projections of loading vectors, it can be concluded that all descriptors have almost the same impact on PC1 and PC2, while at the same time the descriptors do not demonstrate distinct positive or negative influence on PC variables.

3.4. Modeling of retention and biological activity

To qualify relationships between factors governing lipophilicity and those that could contribute to the biological activities of the studied analogs, PLS modeling was performed on retention (R_M^0) and lipophilicity data ($\log P_{OW}$), as well as on data of biological activity against the BoNT/A LC, malaria, and EBOV. The number of latent variables was selected on the basis of minimum value of *RMSECV*, as well as the minimum difference between *RMSEC* and *RMSECV* values. The resulting models are summarized in Table 3.

The contribution of descriptors with the strongest influence on chromatographic behavior and biological activity was analyzed using variable importance in projection scores (VIP). The descriptors included in the final models for lipophilicity, of the BoNT/A LC and malarial strains D6, W2, and C235, are presented in Table 3 in descending order of regression coefficients, with notification of the sign of their contribution on the dependent variable.

The results indicate that the most relevant descriptors influencing lipophilicity are: (1) the index of cohesive interaction in solids (ACxDN:5/SA), (2) predicted octanol/water partition coefficients (QP log $P_{O/W}$), (3) predicted water–gas partition coefficients (QP log P_W), (4) predicted aqueous solubility (QP log S), (5) human serum albumin binding prediction (QP log K_{hsa}), (6) predicted octanol–gas partition coefficients (QP log P_{oct}), (7) the van der Waals surface area of polar nitrogen and oxygen atoms (PSA), (8) total solvent accessible surface area (SASA) and the hydrophobic component of the SASA (FOSA), and (9) molecular volume. Considering the sign of the regression coefficients, it can be concluded that the polarity of the investigated compounds, *i.e.*, their abilities to engage in hydrophilic interactions, negatively contribute to R_M^0 values. The ACxDN:5/SA term represents the relationship: (AccptHB($\sqrt{\text{DonorHB}}$)/(SA)) (AccptHB, DonorHB,—which is an estimate of the number of hydrogen bonds that would be accepted (or donated) by the compounds from (or to) water molecules/surface area (SA)), and indicates the measure of the specific interactions with mobile phase. QP log S, QP log P_W, QP log P_{oct}, and PSA are descriptors of polar interactions between the solute and the mobile phase. Higher QP log values, as well as PSA, are indicative of weaker retention. In contrast, descriptors such as QP log $P_{O/W}$, SASA, and FOSA describe the non-polar properties of the compounds and the ability to engage in hydrophobic (dispersive) interactions with the stationary phase, and thus positively contribute to retention. The volume of the molecule has a positive influence on retention, indicating that bulky compounds are strongly retained on the stationary phase. These molecular descriptors also exist in the QSPR model, and show the same influence on the log P_{OW} as on retention.

Table 3
Results obtained *via* PLS analysis.

Dependent variable	Statistical performance of the model				Molecular descriptors included in the model
	R^2_{cal}	R^2_{CV}	*RMSEC*	*RMSECV*	
R_M^0	0.9468	0.9094	0.142	0.185	QP log P_W (−), QP log K_{hsa} (+), ACxDN:5/SA (−), QP log $P_{O/W}$ (+), QP log S (−), PSA (−), SASA (+), FOSA (+), volume (+)
log P_{OW}	0.9381	0.9278	0.182	0.197	QP log P_W (−), ACxDN:5/SA (−), QP log P_{oct} (−), QP log K_{hsa} (+), PSA (−), QP log $P_{O/W}$ (+), QP log S (−)
BoNT LC%	0.9113	0.8799	0.022	0.025	AccptHB (−), EA (−), IP (−), LUMO and HOMO energy (+), mol. electronegativity (+), FISA (+), PISA (+), DonorHB (+)
D6 IC_{50}	0.8864	0.8765	0.356	0.341	EA (−), IP (−), AccptHB (−), LUMO and HOMO energy (+), mol. electronegativity (+), FISA (+), DonorHB (+), FOSA (−)
W2 IC_{50}	0.9506	0.9302	0.179	0.213	AccptHB (−), FISA (+), DonorHB (+), PISA (+), potential energy (−), mol MW (−), volume (−), total atom self permeability (+), PSA (+)
C235 IC_{50}	0.9187	0.9112	0.253	0.265	AccptHB (−), FISA (+), DonorHB (+), PISA (+), LUMO and HOMO energy (+), mol. electronegativity (+), potential energy (−), mol MW (−), PSA (+)

Quantitative relationships between each type of analyzed biological activity and structural descriptors support the assumed mechanisms of action of the studied compounds. Based on the calculated VIP scores, negative AccptHB and positive DonorHB are present in all four models, and consequently represent a favorable influence on the measure of activity. Descriptors such as HOMO and LUMO energy, molecular electronegativity, and the hydrophilic component of SASA (FISA) are significant for compound activities as they relate to the BoNT/A LC, and malarial strains D6 and C235, whereas the π component of SASA (PISA) segregates activity between malarial strain D6 and activities against the BoNT/A LC and malarial strains W2 and C235. Moreover, descriptors such as potential energy, molecular weight (MW), and PSA are present in the models for malarial strain W2 and C235 activity prediction, whereas ionization potential (IP) and electron affinity (EA) are discriminative for the BoNT/A LC model and malarial strains D6. It is also interesting to note that model descriptors for activity against malarial strains D6 and W2 are significantly different.

For BoNT/A LC inhibition, the proposed mechanism of action is direct, competitive inhibition of the enzyme's metalloprotease component [12]. Therefore, the descriptors AccptHB and DonorHB are indicative atom–atom level interactions that occur between the small molecules' nitrogen containing functional groups and residues composing the enzyme's substrate binding cleft. Specifically, the substrate binding cleft of the BoNT/A LC possesses several amino acid residues (*e.g.*, Glu55, Glu164, Glu252, Ser259, Tyr366, Asp370) that are positioned in the vicinity of enzymes Zn(II) catalytic engine. These residues could act as hydrogen bond donors and/or acceptors, and may serve as a binding contacts for 1,7-DAAC derivatives, thereby positioning the molecules in such a manner the hydrolytic potential of the enzyme is inhibited.

The proposed mechanism of antimalarial activity involves binding of the derivatives' core diazachrysene ring systems, which act as bioisostere of chloroquine [12] to hematin ((Fe(III)FPIX), a toxic biproduct released in the parasite's food vacuole during feeding). Specifically, this binding suspends the production of malaria black (the molecular crystal used for hematin clearance), and ultimately leads to parasite death. Consequently, the influence of the AccptHB and DonorHB descriptors emphasizes the importance of the compound's nitrogen-containing components in terms of properly positioning the ligands so that the necessary geometry for interacting with monomeric hematin is achieved [12]. Additionally, it is well-documented that mutations in *P. falciparum* chloroquine resistant transporter (PfCRT), multi-drug resistance protein 1 (PfMDR1), and multi-drug resistance-associated protein (PfMRP) are responsible for the development of resistance to traditional antimalarial drug chloroquine and its analogs [29]. Hence, the contributions of the AccptHB and DonorHB descriptors appear to be of additional importance to the observed antimalarial activities of the 1,7-DAAC-based compounds, especially against CQ-resistant strains (Table 1). The hydrophilic and π components of SASA (FISA and PISA) represent the contribution of hydrophilic and hydrophobic interactions in protein–ligand complexes. In order to provide antimalarial activity a key step is the positioning of the 1,7-DAAC aromatic moiety on one side of hematin and binding with dispersive forces, such that further interactions with another hematin molecule are obstructed. Therefore, the role of the PISA descriptor is obvious.

The relationship between the antiviral inhibition for EBOV provided by select 1,7-DAAC derivatives (primary screen data, % inhibition at 20 μM conc.) and structural descriptors was also analyzed by PLS. However, the obtained model was not of satisfactory statistical quality to provide quantitative SARs, but may qualitatively indicate which descriptors contribute to antiviral activity. Based on the VIP scores, the following molecular descriptors were identified as the most influential factors with respect to EBOV inhibition: PISA, computed dipole moment of the molecule, IP, EA, ACxDN:5/SA, number of likely metabolic reactions (metab), QP log P_W, QP log P_{HERG}, and QP log K_{hsa}, in descending order of coefficient values in the regression graphs, respectively. Regression vectors of the obtained models indicate that descriptors IP, EA, ACxDN:5/SA, metab, QP log P_W, and QP log P_{HERG} influence EBOV inhibitory activity in a negative manner, while the rest of the descriptors display a significant, positive effect.

The activity models against all three pathogens, and QSRR models, indicate that both compound retention on the RPC system and specific biological activity are influenced by different structural features. Regression vectors obtained for the QSR(P)R models are opposite to those for the QSARs (Table 3). For example, molecular descriptors that appeared in the QSR(P)Rs determine the ability of compounds to diffuse from a dilute solution outside of the cell to a particular site inside the cell. These parameters can be useful for elucidating interactions that occur during the transport of compounds to their sites of action, while QSAR models indicate molecular descriptors that account for the interactions of compounds with specific sites within the cells.

Based on the above observations, all predicted partition coefficients were excluded from the set of descriptors and replaced with experimentally obtained log P_{OW} values, and then correlated with the compounds' biological activities to verify the influence of lipophilicity on their mechanisms of action. Following, it was found that all of the modified PLS models were in good agreement with previously calculated models with identical statistical parameters, thereby further indicating the quality of the models. Additionally, the most important descriptors from the VIP scores were equivalent in both cases. Therefore, log P_{OW} values are not included in the final models, strongly suggesting that the biological activities of the 1,7-DAAC derivatives are not determined by their lipophilicity, but rather, by specific interactions with their respective sites of action. Such results are in accordance with our previous work in which the QSRR/QSAR studies were performed on bis-steroidal tetraoxanes. Specifically, results from this study indicated that different structural descriptors correlate times of retention on a chromatographic system with biological activity [6].

4. Conclusion

The presented work focused on the determination of the physicochemical properties, retention parameter, R_M^0, partition coefficient, log P_{OW}, and pK_a values of thirteen biologically active 1,7-DAAC derivatives, as well as the determination of molecular descriptors that appear to affect both their RPC behavior and biological activities against three unrelated pathogens.

Determined lipophilicity parameters were in accordance with the structural characteristics of the examined derivatives. pK_a values were potentiometrically determined and calculated using Epik module. According to experimentally determined pK_{a1}–pK_{a4} values for representative derivative **12**, distribution of the species within a physiologically relevant pH range was calculated.

PCA and HCA, followed by PLS, were used to select descriptors that best describe behavior of the investigated compounds in chromatographic and biological systems, and to quantify their influences *via* models that may be used to predict the behavior of new derivative designs. QSR(P)R models revealed the importance of descriptors related to the hydrophobic components of the examined compounds, such as predicted partition coefficients, hydrophobic components of surface area. QSARs indicated the importance of the specific interactions of compounds with binding sites within the cells, which describe compound polarity, distribution of electron density, and proton donating/accepting abilities. The obtained equations are based on physically meaningful parameters, and provide a quantitative means for explaining compound

lipophilicity and activity, *i.e.*, the chromatographic and biological behavior of the investigated compounds. Finally, a qualitative SAR model for 1,7-DAAC activity against EBOV was identified, and provides insights into the parameters influencing the effects of the compounds on this pathogen.

Acknowledgements

This research was supported by (1) the Ministry of Education and Science of Serbia (Grant No. 172008) and (2) NATO's Public Diplomacy Division in the framework of "Science for Peace" project SfP983638. For J.C.B., in compliance with SAIC-Frederick, Inc. contractual requirements: this project has been funded in whole or in part with federal funds from the National Cancer Institute, National Institutes of Health (USA), under Contract No. HHSN261200800001E. The content of this publication does not necessarily reflect the views or policies of the Department of Health and Human Services (USA), nor does the mention of trade names, commercial products, or organizations imply endorsement by the US Government. SARvisionPLUS version 3.1 (Altoris, ChemApps, La Jolla, USA) was used as a tool for navigation through vast chemical information and as an aide for identification of structure–property relationships generated during preparation of current publication.

Appendix A. Supplementary data

Supplementary data associated with this article can be found, in the online version, at http://dx.doi.org/10.1016/j.jpba.2012.08.025.

References

[1] H. Wan, A.G. Holmen, High throughput screening of physicochemical properties and in vitro ADME profiling in drug discovery, Comb. Chem. High T. Scr. 12 (2009) 315–329.
[2] M.P. Gleeson, A. Hersey, D. Montanari, J. Overington, Probing the links between in vitro potency, ADMET and physicochemical parameters, Nat. Rev. Drug Discov. 10 (2011) 197–208.
[3] R.B. Silverman, The Organic Chemistry of Drug Design and Drug Action, Elsevier Academic Press, Burlington, 2004, pp. 27–34.
[4] OECDiLibrary, OECD Guidelines for the Testing of Chemicals, Section 1: Physical–chemical Properties, 2011, http://www.oecd-ilibrary.org/environment/test-no-117-partition-coefficient-n-octanol-water-hplc-method_9789264069824-en;jsessionid=7m94n4k803g83.delta.
[5] F.Lj. Andrić, J.Đ. Trifković, A.D. Radoičić, S.B. Šegan, Ž.Lj. Tešić, D.M. Milojković-Opsenica, Determination of the soil–water partition coefficients (log KOC) of some mono- and poly-substituted phenols by reversed-phase thin-layer chromatography, Chemosphere 81 (2010) 299–305.
[6] S. Šegan, F. Andrić, A. Radoičić, D. Opsenica, B. Šolaja, M. Zlatović, D. Milojković-Opsenica, Correlation between structure, retention and activity of cholic acid derived cis–trans isomeric bis-steroidal tetraoxanes, J. Sep. Sci. 34 (2011) 2659–2667.
[7] J. Trifković, F. Andrić, P. Ristivojević, D. Andrić, Ž.Lj. Tešić, D.M. Milojković-Opsenica, Structure–retention relationship study of arylpiperazines by linear multivariate modelling, J. Sep. Sci. 33 (2010) 2619–2628.
[8] R.F. Cookson, The determination of acidity constants, Chem. Rev. (1974) 5–28.
[9] A. Avdeef, B. Testa, Physicochemical profiling in drug research: a brief survey of the state-of-the-art of experimental techniques, Cell. Mol. Life Sci. 59 (2002) 1681–1689.
[10] R. Kaliszan, Structure and Retention in Chromatography. A Chemometric Approach, Harwood Academic Publishers, Amsterdam, 1997, pp. 127–152.
[11] M. Koba, T. Bączek, M.P. Marszałł, Importance of retention data from affinity and reverse-phase high-performance liquid chromatography on antitumor activity prediction of imidazoacridinones using QSAR strategy, J. Pharm. Biomed. Anal. 64-65 (2012) 87–93.
[12] I. Opsenica, J.C. Burnett, R. Gussio, D. Opsenica, N. Todorović, C.A. Lanteri, R.J. Sciotti, M. Gettayacamin, N. Basilico, D. Taramelli, J.E. Nuss, L. Wanner, R.G. Panchal, B.A. Šolaja, S. Bavari, A chemotype that inhibits three unrelated pathogenic targets: the Botulinum neurotoxin serotype a light chain, *P. falciparum* malaria, and the Ebola Filovirus, J. Med. Chem. 54 (2011) 1157–1169.
[13] A.R. Hermone, J.C. Burnett, J.E. Nuss, L.E. Tressler, T.L. Nguyen, B.A. Šolaja, J.V. Vennerstrom, J.J. Schmidt, P. Wipf, S. Bavari, R. Gussio, Three-dimensional database mining identifies a unique chemotype that unites structurally diverse botulinum neurotoxin serotype a inhibitors in a three-zone pharmacophore, ChemMedChem 3 (2008) 1905–1912.
[14] C. Hansch, A. Leo, D. Hoekman, Exploring QSAR. Hydrophobic, Electronic, and Steric Constants, ACS Professional Reference Book, American Chemical Society, Washington, DC, 1995, pp. 1–216.
[15] H.M. Irving, M.G. Miles, L.D. Pettit, A study of some problems in determining the proton disassociation constant of complexes by potentiometric titration using a glass electrode, Anal. Chim. Acta 38 (1967) 475–488.
[16] P. Gans, A. Sabatini, A. Vacca, Investigation of equilibria in solution. Determination of equilibrium constants with the HYPERQUAD suite of programs, Talanta 43 (1996) 1739–1753.
[17] C. Hansch, A. Leo, Substituent Constants for Correlation Analysis in Chemistry and Biology, Wiley, New York, 1979.
[18] Epik, versEpik, version 2.2, Schrödinger, LLC, New York, NY, 2011.
[19] I. Kolossváry, W.C. Guida, Low-mode conformational search elucidated: application to C39H80 and flexible docking of 9-deazaguanine inhibitors into PNP, J. Comput. Chem. 20 (1999) 1671–1684.
[20] E. Polak, G. Ribiere, Note sur la convergence de méthodes de directions conjuguées, Revenue Francaise Informat. Recherche Operationelle, Serie Rouge 3 (1969) 35–43.
[21] G.B. Rocha, R.O. Freire, A.M. Simas, J.J.P. Stewart, RM1. A reparameterization of AM1 for H, C, N, O, P, S, F, Cl, Br, and I, J. Comput. Chem. 27 (2006) 1101–1111.
[22] M. Daszykowski, S. Serneels, K. Kaczmarek, P. Van Espen, C. Croux, B. Walczak, TOMCAT A MATLAB toolbox for multivariate calibration techniques, Chemom. Intell. Lab. Syst. 85 (2007) 269–277.
[23] Q.-S. Xu, Y.-Z. Liang, Monte Carlo cross-validation, Chemom. Intell. Lab. Syst. 56 (2001) 1–11.
[24] R.G. Brereton, Chemometrics, Data Analysis for the Laboratory and Chemical Plant, Wiley, Chichester, England, 2003, pp. 297–323.
[25] K. Varmuza, P. Filzmaser, Introduction to Multivariate Statistical Analysis in Chemometrics, CRC Press/Taylor & Francis Group, Boca Raton, 2008.
[26] M. Natić, R. Marković, D. Milojković-Opsenica, Ž. Tešić, Structure–retention relationship study of diastereomeric (Z)- and (E)-2-alkylidene-4-oxothiazolidines, J. Sep. Sci. 30 (2007) 2241–2248.
[27] S.R. Hawley, P.G. Bray, B.K. Park, S.A. Ward, Amodiaquine accumulation in *Plasmodium falciparum* as a possible explanation for its superior antimalarial activity over chloroquine, Mol. Biochem. Parasit. 80 (1996) 15–25.
[28] S. Parapini, N. Basilico, E. Pasini, T.J. Egan, P. Olliaro, D. Taramelli, D. Monti, Standardization of the physicochemical parameters to assess *in vitro* the β-hematin inhibitory activity of antimalarial drugs, Exp. Parasitol. 96 (2000) 249–256.
[29] A. Ecker, A.M. Lehane, D.A. Fidock, Molecular markers of plasmodium resistance to antimalarials, in: H.M. Staines, S. Krishna (Eds.), Treatment and Prevention of Malaria: Antimalarial Drug Chemistry, Action and Use, Springer, Basel, 2012, pp. 249–280.